

Piano-Stool Iron(II) Complexes as Probes for the Bonding of *N*-Heterocyclic Carbenes: Indications for π -Acceptor Ability

Laszlo Mercs,[†] Gaël Labat,[‡] Antonia Neels,[‡] Andreas Ehlers,[§] and Martin Albrecht^{*,†}

Department of Chemistry, University of Fribourg, Ch. du Musée 9, CH-1700 Fribourg, Switzerland,
Institute of Microtechnology, University of Neuchâtel, Rue Emile Argand 11,
CH-2009 Neuchâtel, Switzerland, and Scheikundig Laboratorium, Vrije Universiteit van Amsterdam,
De Boelelaan 1083, 1081 HV Amsterdam, The Netherlands

A series of new piano-stool iron(II) complexes comprising mono- and bidentate chelating *N*-heterocyclic carbene ligands [Fe(cp)(CO)(NHC)(L)]X have been prepared and analyzed by spectroscopic, electrochemical, crystallographic, and theoretical methods. Selectively substituting the L site with a series of ligands going from carbene to pyridine to CO suggests that CO is the strongest π acceptor, while the behavior of pyridine and carbene is nearly identical. This suggests that in these complexes comprising an electron-rich iron(cp)(carbene) fragment, *N*-heterocyclic carbenes are not pure σ donors but also moderate π acceptors. Theoretical calculations support this bonding model and indicate charge saturation at the metal as key for π back-bonding to *N*-heterocyclic carbenes. On the basis of voltammetric measurements, the Lever electrochemical parameter of these carbenes has been determined: $E_L = +0.29$. Systematic substitution of the wingtip groups of the carbene revealed only subtle changes in the electronic properties of the iron center, thus providing a suitable methodology for ligand-induced fine-tuning of the coordinated metal.

Introduction

The discovery of *N*-heterocyclic carbenes (NHCs) as ligands for transition metals has greatly stimulated the development of efficient catalysts.¹ Often, these carbene complexes surpass the activity of their corresponding phosphine analogues.² Their catalytic performance may be optimized by ligand tuning, since steric and electronic influences of a large number of ligands have been tabulated. In organometallic chemistry, Tolman's electronic parameters (ν) are typically used,³ while in coordination chemistry ligands are more often classified according to Lever's electrochemical parameters (E_L).⁴ Recently, a theoretical model has been proposed, which relates these two parameters via computed electronic parameters. This allows the classification also of ligands that have not been considered thus far.⁵ For example, NHCs have been suggested to be some of the

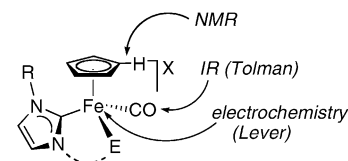


Figure 1. Direct and indirect probes for ligand tuning in Fe(II) carbene complexes.

strongest neutral donors available to date, having donor strengths only slightly weaker than anionic I^- . Some IR investigations on Rh and Ir complexes⁶ confirmed the theoretical prediction that heteroatom-stabilized carbenes are generally stronger ligands than the most basic phosphines.

We were interested to combine the probes of Lever and Tolman in order to classify the basicity of carbenes quantitatively. Half-sandwich iron carbonyl complexes are particularly attractive, as they combine a redox-active Fe^{II} center and a CO ligand for Lever- and Tolman-type parametrization, respectively. This allows the quantification of the effects of both the wingtip group R and the donor E. Due to the conformational rigidity of these complexes, the ligand basicity may be measured eventually also by NMR spectroscopy, using the carbon and proton nuclei of the cyclopentadienyl (cp) ligand as probes.

Here we report on a series of new iron(II) carbene complexes in which the ligands can be varied systematically (Figure 1). Steric effects of the wingtip groups have been investigated through substitution of R = Me to R = *i*Pr, and electronic influences by including mesityl (Mes)-substituted NHCs. In addition, variation of the donor site E from carbene to different ligands such as pyridine, iodide, and CO allows a quantitative

* To whom correspondence should be addressed. E-mail: martin.albrecht@unifr.ch. Fax: +41-263009738.

[†] University of Fribourg.

[‡] University of Neuchâtel.

[§] Vrije Universiteit van Amsterdam.

(1) (a) Wanzlick, H.-W.; Schönherr, H.-J. *Angew. Chem., Int. Ed. Engl.* **1968**, *7*, 141. (b) Öfele, K. *J. Organomet. Chem.* **1968**, *12*, P42. (c) Arduengo, A. J.; Harlow, R. L.; Kline, M. *J. Am. Chem. Soc.* **1991**, *113*, 361. (d) Bourissou, D.; Guerret, O.; Gabbai, F. P.; Bertrand, G. *Chem. Rev.* **2000**, *100*, 39. (e) Herrmann, W. A. *Angew. Chem., Int. Ed.* **2002**, *41*, 1290. (f) César, V.; Bellemin-Lapomnaz, S.; Gade, L. H. *Chem. Soc. Rev.* **2004**, *33*, 619. (g) Cavell, K. J.; McGuinness, D. S. *Coord. Chem. Rev.* **2004**, *248*, 671.

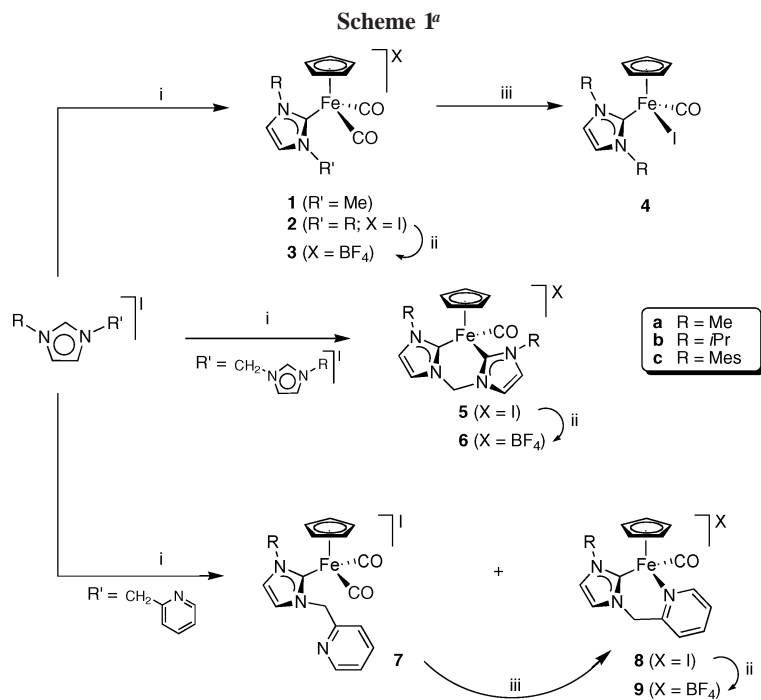
(2) Scholl, M.; Trnka, T. M.; Morgan, J. P.; Grubbs, R. H. *Tetrahedron Lett.* **1999**, *40*, 2247. (b) Huang, J.; Schanz, H. Z.; Stevens, E. D.; Nolan, S. P. *Organometallics* **1999**, *18*, 5375. (c) Perry, M. C.; Cui, X.; Powell, M. T.; Hou, D.-R.; Reibenspies, J. H.; Burgess, K. *J. Am. Chem. Soc.* **2003**, *125*, 113. (d) Navarro, O.; Marion, N.; Mei, J.; Nolan, S. P. *Chem. Eur. J.* **2006**, *12*, 5142. (e) O'Brien, C. J.; Kantchev, E. A. B.; Valente, C.; Hadei, N.; Chass, G. A.; Lough, A.; Hopkinson, A. C.; Organ, M. G. *Chem. Eur. J.* **2006**, *12*, 4743.

(3) Tolman, C. A. *Chem. Rev.* **1977**, *77*, 313.

(4) (a) Lever, A. B. P. *Inorg. Chem.* **1990**, *29*, 1271. (b) Lever, A. B. P. *Inorg. Chem.* **1991**, *30*, 1980.

(5) Perrin, L.; Clot, E.; Eisenstein, O.; Loch, J.; Crabtree, R. H. *Inorg. Chem.* **2001**, *40*, 5806.

(6) (a) Chianese, A. R.; Li, X.; Janzen, M. C.; Faller, J. W.; Crabtree, R. H. *Organometallics* **2003**, *22*, 1663. (b) Viciano, M.; Mas-Marza, E.; Sanau, M.; Peris, E. *Organometallics* **2006**, *25*, 3063.



^a Reagents and conditions: (i) KOtBu, thf, RT 1.5 h or BuLi, thf, $-78\text{ }^\circ\text{C}$; then $[\text{FeI}(\text{cp})(\text{CO})_2]$, toluene, RT, 20 h; (ii) AgBF_4 , CH_2Cl_2 , RT, 3 h; (iii) $h\nu$, CH_2Cl_2 , 16 h.

comparison of the donor properties of these ligands in a well-defined environment.

Our results unexpectedly suggest a similar basicity of NHCs and pyridine ligands in these piano-stool iron(II) carbene complexes. Given the stronger σ donation of NHC versus pyridine, the π -acceptor properties of NHCs must be at least as significant as in pyridines and not, as often quoted,^{1d,e} negligible. Theoretical studies on these complexes provide further insight in the carbene bonding mode and reveal significant iron-to-carbene π back-bonding interactions when the metal center is electron-rich.⁷ In addition, the ligand basicity in the Fe complexes investigated shows very little dependence on the wingtip groups, which corroborates previous studies on square-planar complexes.⁸ These results may be particularly relevant for identifying ligand positions that affect the ligand donor properties and hence the catalytic activity of the coordinated metal center.

Results and Discussion

Synthesis of Fe Carbene Complexes. Iron(II) complexes containing a monodentate NHC ligand have been prepared previously by Lappert and co-workers in the course of their pioneering studies on the reactivity of electron-rich enetetramines⁹ and by heterocycle formation at the metal.¹⁰ Since both these methods provide only restricted access to chelated

complexes, we have applied a free carbene route according to a recently established procedure (Scheme 1).¹¹ Deprotonation of the imidazolium salt with a strong base such as KOtBu or *n*BuLi gave the corresponding carbene, which was metalated in situ with $[\text{FeI}(\text{cp})(\text{CO})_2]$ as iron(II) precursor. The formed complexes **1–9** are air-stable when kept in the solid state for several weeks. In CDCl_3 solution, they decompose to a paramagnetic compound typically within a few hours. In DMSO or acetone solution, the cationic monodentate carbene complexes **1** and **2** gradually lose CO to form the corresponding neutral complexes. This reaction is accelerated by UV irradiation and is accompanied by a characteristic color change of the complexes from yellow to green.

Complexation with picolyl-carbenes gave mixtures of two compounds. Spectroscopic analyses identified these products as the monodentate coordinating carbene complex **7** ($\nu_s = 2049\text{ cm}^{-1}$, $\nu_{\text{as}} = 2002\text{ cm}^{-1}$) and the desired chelate **8** ($\nu = 1960\text{ cm}^{-1}$).¹² UV irradiation of the product mixture induced CO dissociation in **7**, thus affording pure **8**. Efforts to prepare **7** selectively by performing the metalation under strict exclusion of light failed, and instead mixtures of **7** and **8** were obtained again. Similarly, exposure of **8** to excess CO (up to 2 bar) did not induce pyridine dissociation.

Formation of the desired complexes is indicated by the expected imidazolium/cp proton ratio in the pertinent ^1H NMR spectra. Chelation of the bidentate dicarbene ligand in **5** and the pyridine-carbene in **8** is evident from the two AX doublets

(7) On the basis of computational studies, the relevance of π interactions in carbene bonding has been discussed controversially. For examples, see: (a) Tafipolsky, M.; Scherer, W.; Öfele, K.; Artus, G.; Pedersen, B.; Herrmann, W. A.; McGrady, G. S. *J. Am. Chem. Soc.* **2002**, *124*, 5865. (b) Hu, X.; Tang, Y.; Gantzel, P.; Meyer, K. *Organometallics* **2003**, *22*, 612. (c) Lee, M.-T.; Hu, C.-H. *Organometallics* **2004**, *23*, 976. (d) Nemcsok, D.; Wichmann, K.; Frenking, G. *Organometallics* **2004**, *23*, 3640. (e) Scott, N. M.; Dorta, R.; Stevens, E. D.; Correa, A.; Cavallo, L.; Nolan, S. P. *J. Am. Chem. Soc.* **2005**, *127*, 3516.

(8) (a) Dorta, R.; Stevens, E. D.; Scott, N. M.; Costabile, C.; Cavallo, L.; Hoff, C. D.; Nolan, S. P. *J. Am. Chem. Soc.* **2005**, *127*, 2485. (b) Scott, N. M.; Nolan, S. P. *Eur. J. Inorg. Chem.* **2005**, 1815.

(9) (a) Cetinkaya, B.; Dixneuf, P.; Lappert, M. F. *J. Chem. Soc., Dalton Trans.* **1974**, 1827. (b) Lappert, M. F. *J. Organomet. Chem.* **1972**, 358, 185.

(10) (a) McCormick, F. B.; Angelici, R. J. *Inorg. Chem.* **1979**, *18*, 1231. (b) Rieger, D.; Lotz, S. D.; Kernbach, U.; André, C.; Bertran-Nadal, J.; Fehlhammer, W. P. *J. Organomet. Chem.* **1995**, *491*, 135.

(11) (a) Raubenheimer, H. G.; Scott, F.; Cronje, S.; Rooyen, P. H.; Psotta, K. *J. Chem. Soc., Dalton Trans.* **1992**, 1009. (b) Buchgraber, P.; Toupet, L.; Guerschais, V. *Organometallics* **2003**, *22*, 5144.

(12) Formation of a neutral carbene complex comprising a coordinated iodide and a monodentate coordinating carbene with a dangling picolyl wingtip substituent has been discarded on the basis of variable-temperature NMR experiments. No indication of a dynamic behavior due to an interconversion to the chelating complex with a noncoordinating iodide anion has been observed in the -80 to $+20\text{ }^\circ\text{C}$ temperature range (acetone- d_6 solution).

due to the methylene protons. Apparently, the boat-like conformation of the six-membered metallacycle is rigid on the NMR time scale. The CH₃ protons of the *i*Pr wingtip substituents of the chelating ligands appear as two distinct doublets, thus indicating a restricted wingtip rotation about the N–C_{propyl} bond. In the ¹H NMR spectrum of **4b**, four different CH₃ groups appear for the *i*Pr wingtip groups. This suggests that rotation about both the Fe–C_{carbene} and the N–C_{*i*Pr} bonds is slow on the NMR time scale. No coalescence is observed up to 90 °C (DMSO solution), which corresponds to an activation energy $\Delta G^\ddagger > 90 \text{ kJ mol}^{-1}$.^{13,14} In contrast, complex **4a**, containing smaller Me wingtip groups, is fluxional at room temperature. A low-temperature limiting spectrum is reached at $T = -20 \text{ }^\circ\text{C}$, which correlates to an approximate free energy of activation $\Delta G^\ddagger = 59 \text{ kJ mol}^{-1}$ for the rotation of the carbene about the Fe–C bond.¹⁵

Infrared spectroscopy provided valuable information on the donor strength of the carbene ligand. Notably, the CO absorption energies appear to be virtually independent of the wingtip substituents. This points to a rather limited influence of those groups on the electronic properties of the metal center. Interestingly, the CO vibrations in the cationic monocarbene complexes **2** ($\nu_s = 2049$ and $\nu_{as} = 2001 \text{ cm}^{-1}$) are similar to those in the precursor complex [Fe(cp)(CO)₂] (2041 and 1997 cm⁻¹). Hence, the donor strength of the formally neutral carbene ligand to the [Fe(cp)(CO)₂]⁺ fragment is comparable to that of the anionic iodide. When bound to the [Fe(cp)(CO)(carbene)]⁺ fragment, however, iodide is a stronger donor ($\nu = 1935 \text{ cm}^{-1}$ in **4**) than carbenes ($\nu = 1950 \text{ cm}^{-1}$ in **5**). This illustrates that the ligand donor power is not an intrinsic parameter but strongly depends on the metal fragment. The data further suggest a similar donor strength for carbene and pyridine ligands ($\nu = 1960 \text{ cm}^{-1}$ in **8**), the carbene being slightly more donating. Such a conclusion is also supported by the ¹³C NMR resonance frequencies of the cyclopentadienyl carbons, which appear at nearly identical frequencies ($\delta_C 81.9 \pm 0.2$ in **5** vs 82.3 ± 0.1 in **8**).

AgBF₄-mediated exchange of the noncoordinating anion from I to BF₄ afforded complexes **3**, **6**, and **9** in good yields (Scheme 1). As expected for substitutions in the outer coordination sphere, the electronic properties of the metal center are not strongly affected. For example, the IR spectroscopic data for the CO vibrations are identical to those of the parent iodide complexes. In the ¹H NMR spectra, a distinct high-field shift of one heterocyclic and the low-field methylene proton is diagnostic for the anion exchange. This may be explained by weak interactions of acidic ligand protons with the anion.¹⁶ Such interactions are expected to be weak for the soft BF₄⁻ anion ($\delta_H 7.94$ and 6.95 in **6c**, CDCl₃ solution), though stronger for iodide ($\delta_H 8.36$ and 7.97 in **5c**). Notably, no such anion-dependent signal shift is seen when the measurements are performed in polar solvents such as DMSO-*d*₆.

(13) Faller J. W. In *Encyclopedia of Inorganic Chemistry*; King, R. B., Ed.; John Wiley: New York, 2005; p 5270.

(14) Instead, metal dissociation is indicated by the rapid evolution of signals assigned to the imidazolium ligand precursor. Decomposition of **4b** in DMSO-*d*₆ solution is temperature dependent, with $t_{1/2} \approx 24 \text{ h}$ at 25 °C and $t_{1/2} \approx 20 \text{ min}$ at 80 °C.

(15) On the basis of this large energy difference, we have discarded an alternative fluxional process involving ligand dissociation and inversion of configuration at the Fe center. For a discussion on the configurational stability of related complexes, see: (a) Brunner, H.; Wallner, G. *Chem. Ber.* **1976**, 109, 1053. (b) Brunner, H. *Eur. J. Inorg. Chem.* **2001**, 905.

(16) For related ion-pairing effects, see: (a) Dupont, J.; Suarez, P. A. Z.; De, Souza, R. F.; Burrow, R. A.; Kintzinger, J-P. *Chem. Eur. J.* **2000**, 6, 2377. (b) Filipponi, S.; Jones, J. N.; Johnson, J. A.; Cowley, A. H.; Grepioni, F.; Braga, D. *Chem. Commun.* **2003**, 2716.

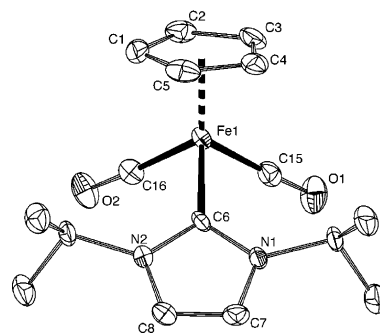


Figure 2. ORTEP representation of **3b** (50% probability ellipsoids; H atoms and BF₄ counterion omitted for clarity).

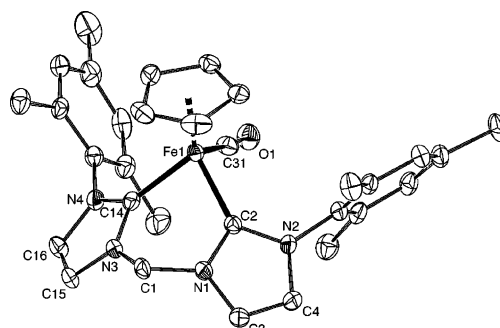


Figure 3. ORTEP representation of the molecular structure of **5c** (30% probability level; H atoms and the nonbonding iodide have been omitted for clarity).

Solid-State Structures. Crystals of **3b** suitable for a structure determination were grown by slow diffusion of Et₂O into a CH₂-Cl₂ solution. The molecular structure (Figure 2) reveals the characteristic piano-stool arrangement of half-sandwich iron complexes. The Fe–carbene bond distance Fe–C6 1.970(3) Å fits well in the 1.97–1.99 Å range of related monodentate carbene–iron bonds in (pseudo-)octahedral geometries^{11,17} yet being significantly shorter than in tetrahedral high-spin complexes (typically 2.07–2.13 Å).¹⁸ The CO–Fe–CO bond angle is 92.8(2)° and thus slightly smaller than the CO–Fe–carbene angles (CO–Fe–C6 94.2(1)° and 94.4(2)°, respectively), presumably due to the steric impact of the carbene ligand.

The molecular structure of **5c** (Figure 3) provides unambiguous evidence for the chelating bonding mode of the dicarbene with a bite angle C2–Fe1–C14 of 86.1(2)°. The metallacycle adopts a boat-like conformation, which is—according to the magnetic inequivalence of these methylene protons—also present in solution. The Fe–C bonds (1.952(5) and 1.955(5) Å) are slightly shorter than in the monocarbene complex **3b** and similar to those in related iron(II) complexes containing chelating carbene ligands.¹⁹ Apparently, the Fe–C bond length in these complexes is determined predominantly by the steric constraints of the chelate rather than being a consequence of the bond strength. Similarly, the CO bond length cannot be used as a probe for the electron donor properties of the carbene ligand. In **5c**, containing two carbene donors, Fe back-bonding into the CO π^* orbital is expected to be larger than in **3b**, with only one carbene ligand. Contrary to this hypothesis, the C–O bond length is shorter in **5c** (1.113(7) Å) than in **3b** (1.142(4) Å).

(17) Capon, J-F.; El, Hassnaoui, S.; Gloaguen, F.; Schollhammer, P.; Talarmin, J. *Organometallics* **2005**, 24, 2020.

(18) (a) Louie, J.; Grubbs, R. H. *Chem. Commun.* **2000**, 1479. (b) Chen, M-Z.; Sun, H-M.; Li, W-F.; Wang, Z-G.; Shen, Q.; Zhang, Y. *J. Organomet. Chem.* **2006**, 691, 2006.

(19) Danopoulos, A. A.; Tsoureas, N.; Wright, J. A.; Light, M. E. *Organometallics* **2004**, 23, 166.

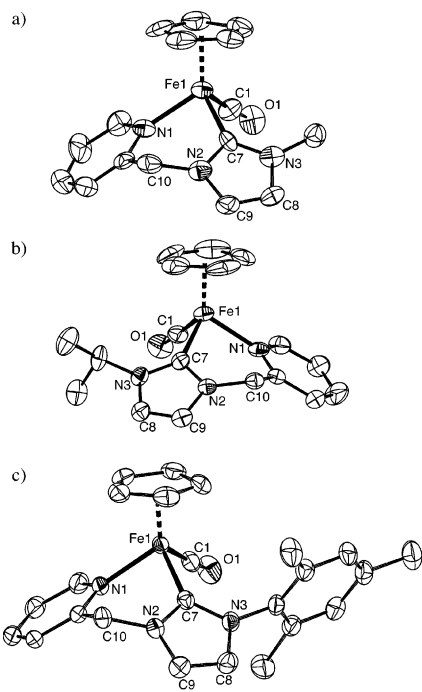


Figure 4. ORTEP representation (50% probability) of the molecular structures of **8a** (a), **8b** (b), and **8c** (c). Hydrogen atoms, cocrystallized solvent molecules, and the noncoordinating iodide ligand have been omitted for clarity. Only one of the two crystallographically independent molecules of **8a** and **8b** are shown.

Notably, the crystal structure of **5c** displays short contacts between the iodide anion and the methylene proton H1A (H1A...I 2.97 Å, C1...I 3.936(5) Å, C1–H1A...I 166°). A similar hydrogen-bonding motif, albeit much weaker, may also exist in solution (vide supra).

The solid-state structures of **8a–c** have been determined in order to study wingtip group effects. The molecular structures of these complexes confirm the *C,N*-bidentate chelating bonding mode deduced from solution measurements (Figure 4a–c). Neither Fe–C_{carbene} nor carbonyl C–O bond length analyses show any correlation for wingtip-dependent iron–carbene bond lengths. The largest differences are seen for the pyridine–carbene bite angle, which is smaller for the mesityl-substituted ligand. This may be due to the conformational rigidity of the mesityl group, since wingtip change from Me (**8a**) to sterically more demanding though flexible *i*Pr (**8b**) does not influence the ligand bite angle similarly.

In all three complexes, short contacts are observed between the noncoordinating iodide anion and the acidic CH₂ protons of the methylene that interlinks the two heterocycles (Table 1). In addition, **8c** reveals C_{cp}–H...O_{CO} hydrogen bonds in the solid state, thus resulting in a dimeric structure (Figure 5). The H...O distance is 2.42 Å and hence rather short, though the carbonyl C–O bond is not exceedingly stretched when compared with **8a** and **8b**, which do not form similar dimers.

Electrochemical Measurements. Electrochemical analysis of the Fe^{III}/Fe^{II} redox potential E^0 offers a useful probe of the ligand basicity.⁴ Thus, low oxidation potentials and hence a better stabilization of iron(III) rather than iron(II) centers is expected for ligands that are strongly donating. Electrochemical measurements have been carried out on the neutral complex **4** and all ionic BF₄ complexes in CH₂Cl₂ containing 0.1 M *n*Bu₄PF₆ as supporting electrolyte. The data are compiled in Table 2 and correspond to standard potentials for fully reversible Fe oxidation, except for **6a**, whose oxidation wave appeared to be

Table 1. Hydrogen Bond Interactions in the Pyridine–Carbene Complexes 8a–c

C–H...X	distance (Å)		angle (deg)	sym translation for X
	H...X	C...X	C–H...X	
8a				
C26–H26B...I2	3.04	3.941(10)	151	–1/2 + x, –3/2–y, z
8b				
C8–H8...I1	3.02	3.957(9)	170	–1 + x, y, z
C10–H10A...I1	3.00	3.930(9)	158	–x, 1–y, 1–z
C26–H26...I2	2.97	3.910(9)	170	–1 + x, –1 + y, z
C28–H28A...I2	3.06	3.980(9)	156	–x, 1–y, –z
8c				
C3–H3...O1	2.42	3.231(3)	143	–1–x, 1–y, –z
C8–H8...I1	2.91	3.824(3)	161	x, 1 + y, z
C10–H10B...I1	2.94	3.925(3)	176	–x, y, 1–z
C13–H13...I1	3.05	3.890(3)	149	1 + x, y, z

Table 2. Vibrational and Electrochemical Data of Fe(II) Complexes

entry	complex	bonding mode	$\nu(\text{CO})^a$	$E_{1/2}$ vs SCE ^b	$E_{1/2}$ vs NHE ^c	E (obs) ^d
1	4a	C-monodentate	1936	+0.48	+0.72	+0.78
2	4b	C-monodentate	1935	+0.46	+0.70	+0.78
3	4c	C-monodentate	1938	+0.41	+0.65	+0.78
4	6a	<i>C,C</i> -bidentate	1950	+1.14 (irrev.) ^f		+1.36
5	6b	<i>C,C</i> -bidentate	1948	+1.10	+1.34	+1.36
6	6c	<i>C,C</i> -bidentate	1956	+1.15	+1.39	+1.36
7	9a	<i>C,C</i> -bidentate	1964	+1.10	+1.34	+1.43
8	9b	<i>C,C</i> -bidentate	1964	+1.16	+1.40	+1.32
9	9c	<i>C,C</i> -bidentate	1966	+1.18	+1.42	+1.32

^a In cm^{–1} measured in CH₂Cl₂. ^b In V vs SCE ($E_{1/2}$ Fc⁺/Fc at +0.46 V), measured in CH₂Cl₂, 0.1 M [Bu₄N][PF₆] electrolyte, sweep rate 200 mV s^{–1}. ^c Calculated based on $E(\text{SCE}) = 0.24$ V. ^d Calculated according to eq 2 with $E_{\text{L}}(\text{NHC}) = +0.29$, $E_{\text{L}}(\text{cp}) = +0.04$. ^e From ref 11b. ^f E_{pa} of irreversible oxidation.

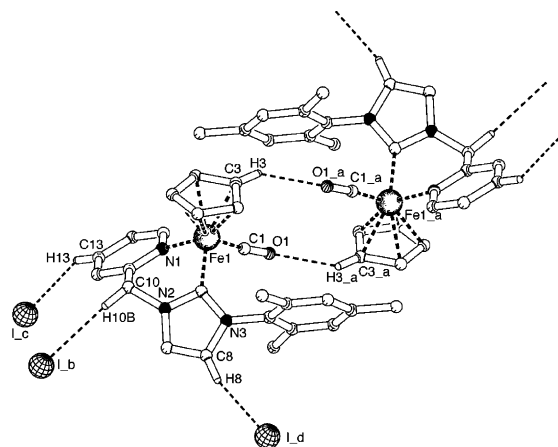


Figure 5. Intermolecular C–H...O hydrogen bonding in **8c** provides a dimeric solid-state structure (C3...O1_a 3.231(3) Å, C3–H3...O1_a 143°). The indices represent the following symmetry translations: $a = -1 - x, 1 - y, -z$; $b = -x, -y, 1 - z$; $c = 1 + x, y, z$; $d = x, 1 + y, z$.

irreversible. In addition, the monocarbene complex **3** did not provide any useful signal. According to our calculations using additive electrochemical ligand parameters, a very high oxidation potential is estimated for Fe oxidation in **3** (1.84 V vs SCE).

As expected, the oxidation potentials for the neutral complexes **4** are significantly lower than for the ionic complexes. Furthermore, the wingtip substituents hardly affect the redox potential. Interestingly, only minor differences between the dicarbene complexes **6** and the pyridine–carbenes **9** are observed. This indicates a similar electronic configuration of all these Fe centers and thus closely related donor properties of carbenes and pyridines in these complexes. Such a conclusion

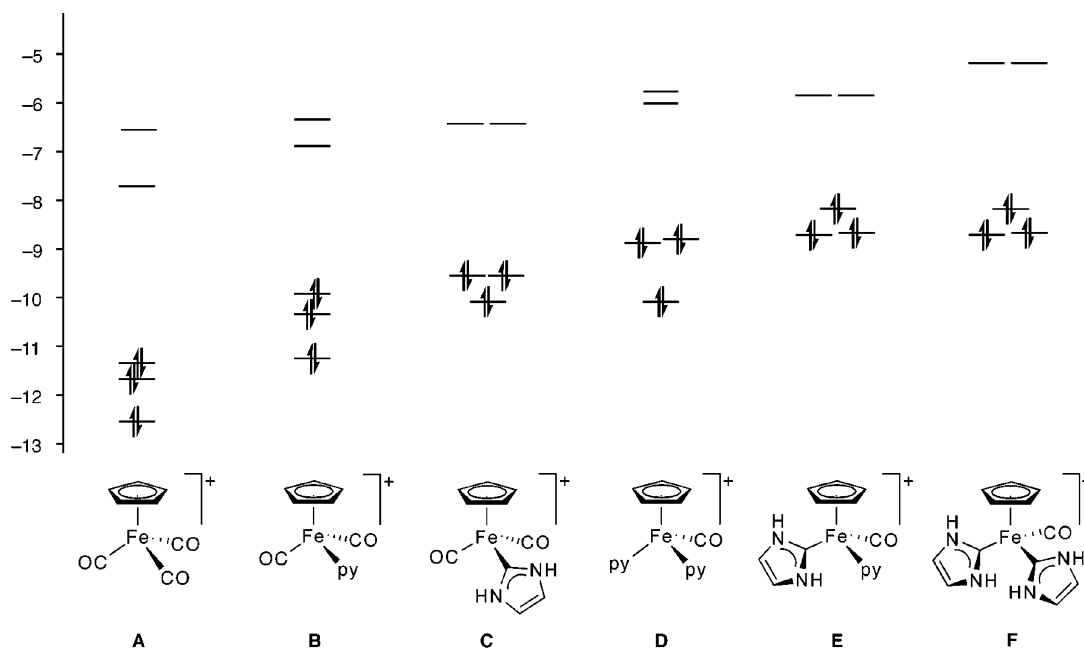


Figure 6. Calculated d orbital energies (in eV) of a series of Fe(cp) complexes.

is also confirmed by the pertinent CO stretching bands of these complexes.²⁰

The electrochemical data help determine Lever's electrochemical parameter E_L for the NHC ligand.⁴ If the ligand contributions are supposed to be additive, that is, if synergistic and steric factors are ignored in a first approximation, the redox potential $E(\text{obs})$ of the low-spin Fe^{III}/Fe^{II} couples follows the least-square equation

$$E(\text{obs}) = 1.11(\sum E_L) - 0.43 \quad (2)$$

The observed standard potentials $E(\text{obs})$ have been corrected to NHE references and averaged for each set of donors. Using eq 2 and the parameters for pyridine ($E_L = +0.25$), iodide ($E_L = -0.24$), and CO ($E_L = +0.99$) gives for *N*-heterocyclic carbenes $E_L = +0.29$ and $E_L = +0.04$ for the cp ligand.²¹ This value may be translated into Hammett substituent parameter σ^{22} and also into Tolman's electronic parameters (ν),³ the latter being frequently used in phosphine chemistry. According to the correlation proposed by Clot and co-workers⁵

$$\nu (\text{cm}^{-1}) = 76.82E_L (\text{V}) + 2049 \quad (3)$$

the Tolman parameter of NHC ligands is determined as $\nu = 2071 \text{ cm}^{-1}$. While this value is at the higher end when compared to previously calculated parameters,⁵ it places carbenes in a donor range similar to that of the most basic phosphines. This corroborates preceding investigations on carbene donor properties using IR stretch vibrations.⁶

The Lever parameters of pyridine and carbene indicate similar ligand donor properties in these iron(II) complexes. Since σ

donation of carbenes is generally accepted to be stronger than for pyridines, our results suggest that also π back-bonding must be stronger in carbenes than in pyridines in order to balance the net charge transfer. This conclusion is particularly relevant when considering that π back-bonding to pyridine ligands is well established.²³

DFT Calculations and Energy Decomposition Analyses. Independent DFT calculations have been carried out for six different [Fe(cp)(CO)L₂]⁺ cations, **A–F**, in the gas phase (Figure 6). While the cations **C**, **E**, and **F** are simplified analogues of the complexes **3**, **6**, and **9**, respectively, the structures **B** and a chelating bipyridine version of **D** have been described in the literature.²⁴ Complex **A** provides a valuable starting point to discuss primary ligand effects.

Geometry optimization gave bond distances that corroborate in most cases the experimental values.²⁵ Exceptions are the calculated structural analogues of **6** and **9**, for which a slightly longer Fe–CO bond distance is predicted from calculations. This may be rationalized by the chelate effect, which organizes the ligand position more rigidly than in a nonchelating system. The scaled IR stretch vibrations corroborate the experimental observations and reflect an increasing ligand basicity, CO \ll pyr \leq NHC.²⁵

In order to further describe the ligand bonding mode, an energy decomposition analysis has been carried out for the cations of type [Fe(cp)(CO)₂L]⁺, **A**, **B**, and **C** (Table 3), with L and [Fe(cp)(CO)₂]⁺ as the two fragments. The calculated bond dissociation energies (BDEs) clearly confirm that the carbene bonding is stronger than that of pyridine and CO, the latter being decreased due to Pauli repulsion. Analysis of the orbital interactions ΔE_{orb} suggests similar π interactions in pyridine and carbene bonding. The π contribution to the Fe–L bond strength in the pyridine-containing cation **B** is 17.8% and for NHC in **C** 15.4%, while in the tricarbonyl cation **A**, this

(20) The ¹H and ¹³C NMR shifts of the cp signals follow a similar trend. While often, NMR chemical shifts are a consequence of various influences, in this case they apparently provide additional support for the electronic configuration at the metal center.

(21) The cp parameter has been confirmed by examining the redox potential of [Fe(cp)(CO)₂]. The measured value (+1.24 V vs SCE) is in good agreement with the calculated potential (+1.30 V vs SCE for $E_L(\text{cp}) = +0.04$ V), indicating that the Lever model is applicable for this kind of complexes. Previously, a slightly higher value has been determined for cp ($E_L = +0.08$ V), albeit based on anodic peak potentials only. See: Jia, G.; Lough, A. J.; Morris, R. H. *Organometallics* **1992**, *11*, 161.

(22) Masui, H.; Lever, A. B. P. *Inorg. Chem.* **1993**, *32*, 2199.

(23) (a) Lindoy, L. F.; Livingstone, S. E. *Coord. Chem. Rev.* **1967**, *2*, 173. (b) Smith, A. P.; Fraser, C. L. In *Comprehensive Coordination Chemistry II*; McCleverty, J. A., Meyer, T. J., Eds.; Elsevier: Oxford, UK, 2004; p 1.

(24) Treichel, P. M.; Shubkin, R. L.; Barnett, K. W.; Reichard, D. *Inorg. Chem.* **1966**, *5*, 1177.

(25) See the Supporting Information for details on the calculations.

Table 3. Energy Decomposition Analyses for the Cations A–C^a

	A	B	C
ΔE_{steric}	33.2	-1.9	-5.4
$\Delta E_{\text{oi}}(a')$	-66.0	-41.2	-66.4
$\Delta E_{\text{oi}}(a'')$	-21.1	-8.9	-12.1
π contribution	48.5%	17.8%	15.4%
BDE	-52.8	-50.0	-81.4

^a In kcal mol⁻¹; π contribution is fraction of $\Delta E_{\text{oi}}(a'')$ /sum(ΔE_{oi}) except for A, where due to symmetry π contribution is a fraction of $2\Delta E_{\text{oi}}(a'')$ /sum(ΔE_{oi}).

Table 4. Charge Transfer in Cations A–C^a

	A	B	C
$\Delta e \sigma$	-0.48	-0.35	-0.62
$\Delta e \pi$	+0.36	+0.04	+0.10
Δe (total)	-0.12	-0.31	-0.52

^a In electrons, negative values indicate charge transfer to the metal (LMCT).

contribution is, as expected, considerably larger (48.5%). These percentages are in line with earlier theoretical investigations²⁶ and represent metal–NHC π interactions that are substantial rather than negligible, as often quoted.^{1d,e} The orbitals that are predominantly involved in these π interactions have been identified as the HOMO of the [Fe(cp)(CO)₂]⁺ fragment as donor and the ligand's aromatic π^* orbitals (LUMO for pyridine and LUMO+1 for NHC) as acceptor orbitals, thus unambiguously suggesting metal-to-ligand back-bonding. On the basis of the amount of transferred charge (Table 4), the NHC ligand is in absolute terms a better π acceptor than pyridine. Yet, the calculations clearly reveal that the metal–carbene bonding is dominated by σ -type ligand-to-metal charge transfer. The σ donation occurs from the carbene lone pair, which is significantly higher in energy (-4.75 eV) than the nitrogen lone pair of pyridine (-5.97 eV). As a result, the energies of the occupied d orbital of the complexes A–F are shifted up to higher levels with increasing number of σ -donor ligands (Figure 6). Obviously, also the π back-bonding of the pyridine and NHC ligands increases in this series (synergistic effect), leading to comparable orbital energies for E and F. This is supported by a further increase of π contribution to 28% for cations [Fe(cp)(L)₃]⁺ (L = py, NHC).

Conclusions

Electrochemical, IR spectroscopic, and theoretical studies of piano-stool Fe(II) carbene complexes have been carried out in order to qualitatively and quantitatively analyze the donor strength of *N*-heterocyclic carbenes. Our studies, which are also supported by NMR chemical shift analyses of the cp spectator ligand, suggest that the donor properties of NHC and pyridine are highly similar when coordinated to the Fe(cp)(carbene) fragment. The Lever electrochemical parameter for carbene ($E_L = 0.29$) has been determined for the first time and relates well to that of pyridine ($E_L = 0.25$). The comparable donor strength of these ligands has been explained by considerable π back-bonding from the electron-rich iron(II) center to the carbene ligand. While metal–carbene π bonding contrasts with the general assumption that carbenes are pure σ donors with negligible π contribution, DFT calculations suggest moderate π -acceptor properties of these NHC ligands. Furthermore,

(26) (a) Frenking, G.; Sola, M.; Vyboishchikov, S. *J. Organomet. Chem.* **2005**, *690*, 6178. (b) Termaten, A. T.; Schakel, M.; Ehlers, A. W.; Lutz, M.; Spek, A. L.; Lammertsma, K. *Chem. Eur. J.* **2003**, *9*, 3577.

wingtip substitution in these piano-stool complexes has only a minor impact on the electronic nature of the central metal. Such groups may therefore be more important for modifying the accessibility rather than the activity of the metal center.

These results corroborate earlier theoretical studies and may contribute to a more refined application of carbenes as ligands. While our results suggest that carbenes do not behave as pure σ -donor ligands, further studies are certainly warranted to generalize this bonding model beyond the iron(II) complexes presented here. Notably, the donor power and π -bonding character depend not just on the ligand but also on the metal fragment, so these results may not be reliably transferable to other systems comprising, for example, electron-poorer metal centers.

Experimental

General Comments. All reactions have been performed using standard Schlenk techniques under a nitrogen atmosphere unless stated otherwise. Toluene, THF, and CH₂Cl₂ were dried by passage through solvent purification columns; all other reagents were used without further purification. The syntheses of the imidazolium salts²⁷ and complexes **2c** and **4c**^{1b} are described elsewhere. All ¹H and ¹³C{¹H} NMR spectra were recorded at 25 °C unless stated otherwise and referenced to residual solvent ¹H or ¹³C resonances (δ in ppm, *J* in Hz). Assignments are based either on distortionless enhancement of polarization transfer (DEPT) experiments or on homo- and heteronuclear shift correlation spectroscopy. IR spectra were recorded on a Mattson 5000 FTIR instrument in CH₂Cl₂ solution. Elemental analyses were performed by the Microanalytical Laboratory of Ilse Beetz (Kronach, Germany). UV irradiation was performed by using a commercial Hg lamp.

Electrochemical Measurements. Electrochemical studies were carried out using an EG&G Princeton Applied Research Potentiostat Model 273A employing a gastight three-electrode cell under an argon atmosphere. A Pt disk with a 3.14 mm² surface area was used as the working electrode and was polished before each measurement. The reference was a saturated calomel electrode (SCE); the counter electrode was a Pt wire. Bu₄NPF₆ (0.1 M) in dry CH₂Cl₂ was used as a base electrolyte with analyte concentrations of approximately 1×10^{-3} M. The redox potentials were measured against the ferrocenium/ferrocene (Fc⁺/Fc) redox couple, which was used as an internal standard ($E_{1/2} = 0.46$ V vs SCE).²⁸

General Procedure for the Preparation of the Monocarbene Complexes 1–3. To a suspension of the imidazolium salt (1.0 molar equiv) in dry THF (15 mL) was added KO^tBu (1.2 molar equiv). After 1 h, this solution was added to a solution of [FeI(cp)(CO)₂] (0.9 molar equiv) in dry toluene (40 mL). After stirring for 16 h, the formed precipitate was separated by centrifugation, washed once with dry toluene (30 mL), and then extracted with dry CH₂Cl₂ (2 × 30 mL). Evaporation of the solvent gave the crude product, which was recrystallized by slow diffusion of Et₂O into a CH₂Cl₂ solution to give an analytically pure sample.

Synthesis of 1a. This complex was prepared from dimethylimidazolium iodide (1.12 g, 5 mmol), KO^tBu (0.67 g, 6 mmol), and [FeI(cp)(CO)₂] (1.44 g, 4.8 mmol). The crude product was obtained as a brownish powder (1.12 g, 58%). ¹H NMR (CDCl₃, 400 MHz): δ 7.32 (s, 2H, im-H), 5.51 (s, 5H, cp), 3.94 (s, 6H, CH₃). ¹³C{¹H} NMR (CDCl₃, 100 MHz): δ 211.4 (CO), 164.0 (im-C²),

(27) (a) Gardiner, M. G.; Herrmann, W. A.; Reisinger, C-P.; Schwarz, J.; Spiegler, M. *J. Organomet. Chem.* **1999**, *572*, 239. (b) Albrecht, M.; Miecznikowski, J. R.; Samuel, A.; Faller, J. W.; Crabtree, R. H. *Organometallics* **2002**, *21*, 3596. (c) Tulloch, A. A. D.; Danopoulos, A. A.; Winston, S.; Kleinhenz, S.; Eastham, G. *J. Chem. Soc., Dalton Trans.* **2000**, 4499. (d) McGuinness, D. S.; Cavell, K. J. *Organometallics* **2000**, *19*, 741. (e) Gründemann, S.; Kovacevic, A.; Albrecht, M.; Faller, J. W.; Crabtree, R. H. *J. Am. Chem. Soc.* **2002**, *124*, 10473.

(28) Connelly, N. G.; Geiger, W. E. *Chem. Rev.* **1996**, *96*, 877.

127.1 (im-C^{4,5}), 87.4 (cp), 40.8 (CH₃). IR (CH₂Cl₂, cm⁻¹): 2048, 2001 ν(CO). Anal. Calcd for C₁₂H₁₃FeIN₂O₂ (399.99): C 36.03, H 3.28, N 7.00. Found: C 35.94, H 3.36, N 7.12.

Synthesis of 1b. This complex was prepared from (*N*-isopropyl-*N'*-methyl)imidazolium iodide (0.50 g, 2 mmol), KO^tBu (0.27 g, 2.4 mmol), and [Fe(cp)(CO)₂] (0.55 g, 1.8 mmol). The crude product was obtained as a yellow powder (1.09 g, 67%). ¹H NMR (CDCl₃, 500 MHz): δ 7.44 (s, 1H, im-H⁴), 7.30 (s, 1H, im-H⁵), 5.48 (s, 5H, cp), 4.86 (septet, 1H, ³J_{HH} = 6.5 Hz, CHMe₂), 3.96 (s, 3H, NCH₃), 1.50 (d, 6H, ³J_{HH} = 6.5 Hz, CH(CH₃)₂). ¹³C{¹H} NMR (CDCl₃, 125 MHz): δ 211.2 (CO), 162.7 (im-C²), 128.4 (im-C⁴), 121.3 (im-C⁵), 87.4 (cp), 53.7 (NCH₃), 41.0 (CHMe₂), 24.0 (CH(CH₃)₂). IR (CH₂Cl₂, cm⁻¹): 2049, 2001 ν(CO). Anal. Calcd for C₁₄H₁₇FeIN₂O₂ (428.05): C 39.28, H 4.00, N 6.54. Found: C 39.22, H 4.10, N 6.58.

Synthesis of 1c. This complex was prepared from (*N*-mesityl-*N'*-methyl)imidazolium iodide (0.66 g, 2 mmol), KO^tBu (0.27 g, 2.4 mmol), and [Fe(cp)(CO)₂] (0.55 g, 1.8 mmol). The crude product was obtained as a green powder (0.41 g, 45%). ¹H NMR (CDCl₃, 400 MHz): δ 7.70 (s, 1H, im), 7.01 (s, 3H, im and mes-H^{3,5}), 5.35 (s, 5H, cp), 4.14 (s, 3H, NCH₃), 2.35 (s, 3H, *p*-CH₃), 1.89 (s, 6H, *o*-CH₃). ¹³C{¹H} NMR (CDCl₃, 100 MHz): δ 210.2 (CO), 167.0 (im-C²), 140.9 (mes-C⁴), 135.8 (mes-C^{2,6}), 135.7 (mes-C¹), 129.8 (mes-C^{3,5}), 128.9, 126.2 (im-C^{4,5}), 87.0 (cp), 41.8 (NCH₃), 21.2 (*p*-CH₃), 18.1 (*o*-CH₃). IR (CH₂Cl₂, cm⁻¹): 2049, 2004 ν(CO). Anal. Calcd for C₂₀H₂₁FeIN₂O₂ (504.14): C 47.65, H 4.20, N 5.56. Found: C 47.76, H 4.16, N 5.50.

Synthesis of 2b. This complex was prepared from (*N,N'*-diisopropyl)imidazolium iodide (0.56 g, 2 mmol), KO^tBu (0.27 g, 2.4 mmol), and [Fe(cp)(CO)₂] (0.55 g, 1.8 mmol). The crude product was obtained as a yellow powder (0.71 g, 87%). ¹H NMR (CDCl₃, 500 MHz): δ 7.41 (s, 2H, im), 5.47 (s, 5H, cp), 4.94 (septet, 2H, ³J_{HH} = 6.7 Hz, CHMe₂), 1.52 (d, 12H, ³J_{HH} = 6.7 Hz, CH(CH₃)₂). ¹³C{¹H} NMR (CDCl₃, 125 MHz): δ 211.0 (CO), 161.4 (im-C²), 122.6 (im-C^{4,5}), 87.3 (cp), 53.7 (CHMe₂), 24.1 (CH(CH₃)₂). IR (CH₂Cl₂, cm⁻¹): 2049, 2001 ν(CO). Anal. Calcd for C₁₆H₂₁FeIN₂O₂ (456.11): C 42.13, H 4.64, N 6.14. Found: C 42.29, H 4.73, N 6.16.

Synthesis of 3b. Complex **2b** (0.20 g, 0.4 mmol) and AgBF₄ (0.10 g, 0.5 mmol) were stirred in dry CH₂Cl₂ (10 mL) under exclusion of light. The solution was stirred for 3 h in the dark, then filtered through Celite. Evaporation of the solvent gave 0.12 g of **7** as a brown powder (69%). ¹H NMR (acetone-*d*₆, 360 MHz): δ 7.83 (s, 2H, im), 5.62 (s, 5H, cp), 5.13 (septet, 2H, ³J_{HH} = 6.6 Hz, CHMe₂), 1.52 (d, 12H, ³J_{HH} = 6.6 Hz, CH(CH₃)₂). IR (CH₂Cl₂, cm⁻¹): 2050, 2002 ν(CO). Anal. Calcd for C₁₆H₂₁BF₄FeN₂O₂ (416.00): C 46.20, H 5.09, N 6.73. Found: C 46.29, H 5.16, N 6.67.

Synthesis of 4a. A solution of **2a** (0.4 g, 1 mmol) in dry CH₂Cl₂ (15 mL) was irradiated for 16 h, upon which the initially brown solution became green. Evaporation of the solvent gave the crude product as a green powder (0.32 g, 86%) that was analytically pure after filtration through Celite and subsequent recrystallization from acetone/pentane. ¹H NMR (acetone-*d*₆, 400 MHz, -20 °C): δ 7.45, 7.34 (2 × s, 2H, im), 4.57 (s, 5H, cp), 4.29, 3.86 (2 × s, 6H, Me). ¹³C{¹H} NMR (acetone-*d*₆, 100 MHz, -20 °C): δ 225.7 (CO), 184.6 (im-C²), 125.5, 125.3 (im-C^{4,5}), 81.0 (cp), 41.9, 39.5 (2 × Me). IR (CH₂Cl₂, cm⁻¹): 1936 ν(CO). Anal. Calcd for C₁₁H₁₃FeIN₂O (371.98): C 35.52, H 3.52, N 7.53. Found: C 35.59, H 3.57, N 7.50.

Synthesis of 4b. This complex was prepared in a manner similar to that for **4a** using **2b** (0.46 g, 1 mmol). Evaporation of the solvent gave the crude product as a green powder (0.40 g, 93%). Filtration through Celite and recrystallization from toluene at -20 °C gave an analytically pure sample. ¹H NMR (CDCl₃, 400 MHz): δ 7.17, 7.06 (2 × s, 2H, im), 6.33, 5.35 (2 × septet, 2H, ³J_{HH} = 6.4 Hz, CHMe₂), 4.45 (s, 5H, cp), 1.60, 1.52, 1.41, 1.28 (4 × d, 12H, ³J_{HH}

= 6.4 Hz, CH(CH₃)₂). ¹³C{¹H} NMR (CDCl₃, 100 MHz): δ 223.8 (CO), 181.9 (im-C²), 120.4, 119.2 (im-C^{4,5}), 79.8 (cp), 54.2, 52.2 (2 × CHMe₂), 24.8, 24.2, 23.9, 23.7 (4 × CH(CH₃)₂). IR (CH₂Cl₂, cm⁻¹): 1935 ν(CO). Anal. Calcd for C₁₅H₂₁FeIN₂O (428.09): C 42.08, H 4.94, N 6.54. Found: C 42.07, H 4.94, N 6.45.

General Procedure for the Preparation of Dicarbene Complexes 5. To a suspension of the corresponding bisimidazolium salt (1 molar equiv) in dry THF (15 mL) was added KO^tBu (2.4 molar equiv) at RT or *n*BuLi (2 molar equiv) at -78 °C. The mixture was stirred at RT for 1 h and then added to a solution of [Fe(cp)(CO)₂] (0.9 molar equiv) in dry toluene (40 mL). After stirring for 16 h, the formed precipitate was separated by centrifugation, washed once with dry toluene (30 mL), and then extracted with dry CH₂Cl₂ (2 × 30 mL). The crude product was obtained by evaporating the solvent.

Synthesis of 5a. This complex was prepared from the methylenedi(*N*-methyl)imidazolium diiodide (1.30 g, 3 mmol), *n*BuLi (1.6 M in hexanes, 3.8 mL, 6 mmol), and [Fe(cp)(CO)₂] (0.82 g, 2.7 mmol). The product was obtained as a brown powder (0.78 g, 64%). Recrystallization from CH₂Cl₂/Et₂O gave an analytically pure sample. ¹H NMR (CDCl₃, 500 MHz): δ 7.96 (d, 2H, ²J_{HH} = 1.7 Hz, im), 7.44 (low-field part of AX d, 1H, ²J_{HH} = 12.8 Hz, CH₂), 7.06 (d, 2H, ²J_{HH} = 1.7 Hz, im), 5.91 (high-field part of AX d, 1H, ²J_{HH} = 12.8 Hz, CH₂), 4.73 (s, 5H, cp), 3.76 (s, 6H, CH₃). ¹³C{¹H} NMR (CDCl₃, 125 MHz): δ 219.2 (CO), 182.9 (im-C²), 124.2, 124.0 (im-C^{4,5}), 82.1 (cp), 62.8 (CH₂), 37.8 (CH₃). IR (CH₂Cl₂, cm⁻¹): 1949 ν(CO). Anal. Calcd for C₁₅H₁₇FeIN₄O (452.07): C 39.85, H 3.79, N 12.39. Found: C 39.93, H 3.85, N 12.43.

Synthesis of 5b. This complex was prepared from methylenedi(*N*-isopropyl)imidazolium diiodide (1.46 g, 3 mmol), *n*BuLi (1.6 M in hexanes, 3.8 mL, 6 mmol), and [Fe(cp)(CO)₂] (0.82 g, 2.7 mmol). The product was obtained as a brown powder (0.75 g, 55%). Recrystallization from acetone/pentane gave an analytically pure sample. ¹H NMR (CDCl₃, 400 MHz): δ 8.08 (d, 2H, ³J_{HH} = 2.2 Hz, im), 7.55 (low-field part of AX d, 1H, ²J_{HH} = 12.9 Hz, CH₂), 7.05 (d, 2H, ³J_{HH} = 2.2 Hz, im), 5.85 (high-field part of AX d, 1H, ²J_{HH} = 12.9 Hz, CH₂), 4.84 (septet, 2H, ³J_{HH} = 6.7 Hz, CHMe₂), 4.69 (s, 5H, cp), 1.46, 1.42 (2 × d, 12H, ³J_{HH} = 6.7 Hz, CH(CH₃)₂). ¹³C{¹H} NMR (CDCl₃, 100 MHz): δ 219.5 (CO), 180.3 (im-C²), 125.3, 118.6 (im-C^{4,5}), 82.1 (cp), 68.3 (CH₂), 52.2 (CHMe₂), 23.8, 23.5 (2 × CH(CH₃)₂). IR (CH₂Cl₂, cm⁻¹): 1948 ν(CO). Anal. Calcd for C₁₉H₂₅FeIN₄O (508.18) × C₃H₆O: C 46.66, H 5.52, N 9.89, Fe 9.86. Found: C 47.17, H 5.27, N 9.86, Fe 9.62.

Synthesis of 5c. This complex was prepared from methylenedi(*N*-mesityl)imidazolium diiodide (1.28 g, 2 mmol), KO^tBu (0.52 g, 4.6 mmol), and [Fe(cp)(CO)₂] (0.55 g, 1.8 mmol). The product was obtained as a greenish powder (0.68 g, 54%). Recrystallization from CHCl₃/pentane gave an analytically pure sample. ¹H NMR (CDCl₃, 500 MHz): δ 8.36 (s, 2H, im), 7.97 (low-field part of AX d, 1H, ²J_{HH} = 12.9 Hz, CH₂), 6.97, 6.94 (2 × s, 4H, mes-H^{3,5}), 6.90 (s, 2H, im), 6.08 (high-field part of AX d, 1H, ²J_{HH} = 12.9 Hz, CH₂), 4.36 (s, 5H, cp), 2.33 (s, 6H, *p*-CH₃), 2.03, 1.70 (2 × s, 12H, *o*-CH₃). ¹³C{¹H} NMR (CDCl₃, 125 MHz): δ 218.8 (CO), 186.2 (im-C²), 139.7 (mes-C¹), 136.3, 135.5, 134.4 (mes-C^{2,4,6}), 129.5, 129.1 (mes-C^{3,5}), 125.2, 124.7 (im-C^{4,5}), 81.7 (cp), 63.0 (CH₂), 21.2 (*p*-CH₃), 18.4, 18.1 (2 × *o*-CH₃). IR (CH₂Cl₂, cm⁻¹): 1956 ν(CO). Anal. Calcd for C₃₁H₃₃FeIN₄O (660.37) × CHCl₃: C 49.29, H 4.40, N 7.19. Found: C 49.23, H 4.48, N 7.05.

General Procedure for the Preparation of BF₄ Complexes 6. All BF₄ salts were prepared from the corresponding iodide complex (1 molar equiv) and AgBF₄ (1.2 molar equiv) in dry CH₂Cl₂ (10 mL) under exclusion of light. The solution was stirred for 3 h in the dark and then filtered through Celite. Evaporation of the solvent gave the desired compound.

Characterization of 6a. ¹H NMR (CDCl₃, 360 MHz): δ 7.66 (s, 2H, im), 7.01 (s, 2H, im), 6.66 (low-field part of AX d, 1H, ²J_{HH} = 12.9 Hz, CH₂), 5.84 (high-field part of AX d, 1H, ²J_{HH} =

12.9 Hz, CH₂), 4.71 (s, 5H, cp), 3.76 (s, 6H, Me). IR (CH₂Cl₂, cm⁻¹): 1950 ν(CO).

Characterization of 6b. ¹H NMR (CDCl₃, 360 MHz): δ 7.70 (d, 2H, ³J_{HH} = 1.8 Hz, im), 7.06 (d, 2H, ³J_{HH} = 1.8 Hz, im), 6.62 (low-field part of AX d, 1H, ²J_{HH} = 13.2 Hz, CH₂), 5.82 (high-field part of AX d, 1H, ²J_{HH} = 13.2 Hz, CH₂), 4.84 (septet, 2H, ³J_{HH} = 6.8 Hz, CHMe₂), 4.68 (s, 5H, cp), 1.46, 1.43 (2 × d, 12H, ³J_{HH} = 6.8 Hz, CH(CH₃)₂). IR (CH₂Cl₂, cm⁻¹): 1948 ν(CO).

Characterization of 6c. ¹H NMR (CDCl₃, 360 MHz): δ 7.94 (s, 2H, im), 6.98–6.90 (m, 7H, im, mes-H,^{3,5} low-field part of CH₂), 6.08 (high-field part of AX d, 1H, ²J_{HH} = 12.7 Hz, CH₂), 4.36 (s, 5H, cp), 2.33 (s, 6H, *p*-CH₃), 2.04, 1.72 (2 × s, 12H, *o*-CH₃). ¹³C-{¹H} NMR (CDCl₃, 90 MHz): δ 219 (CO), 186.3 (im-C²), 139.6 (mes-C¹), 136.4, 135.6, 134.6 (mes-C^{2,4,6}), 129.5, 129.1 (mes-C^{3,5}), 125.1, 124.8 (im), 81.7 (cp), 62.5 (CH₂), 21.3 (*p*-CH₃), 18.5, 18.1 (2 × *o*-CH₃). IR (CH₂Cl₂, cm⁻¹): 1956 ν(CO).

General Procedure for the Preparation of Pyridine–Carbene Complexes 8. The procedure was identical to the preparation of the dicarbene complexes **5**, starting from the imidazolium salt and a slight excess of KO^tBu or 1.0 molar equiv of *n*BuLi. After extraction with CH₂Cl₂ the solution was irradiated for 16 h and subsequently evaporated to dryness to give the desired complex **8**.

Synthesis of 8a. This complex was prepared from (*N*-methyl-*N'*-2-picoly)imidazolium bromide (0.51 g, 2 mmol), KO^tBu (0.25 g, 2.2 mmol), and [FeI(cp)(CO)₂] (0.55 g, 1.8 mmol), affording 0.64 g of product (79%). Recrystallization from CH₂Cl₂/Et₂O gave **8a** as brown crystals. ¹H NMR (CDCl₃, 500 MHz): δ 8.81 (dd, 1H, ³J_{HH} = 5.7 and ⁴J_{HH} = 1.1 Hz, py-H⁶), 8.05 (m, 2H, py-H³ and im), 7.79 (td, 1H, ³J_{HH} = 7.7 and ⁴J_{HH} = 1.6 Hz, py-H⁴), 7.13 (d, 1H, ³J_{HH} = 2.0 Hz, im), 7.12–7.09 (m, 1H, py-H⁵), 6.47 (low-field part of AX d, 1H, ²J_{HH} = 16.1 Hz, CH₂), 5.55 (high-field part of AX d, 1H, ²J_{HH} = 16.1 Hz, CH₂), 4.79 (s, 5H, cp), 3.75 (s, 3H, CH₃). ¹³C-{¹H} NMR (CDCl₃, 125 MHz): δ 219.0 (CO), 181.0 (im-C²), 159.7 (py-C²), 159.1 (py-C⁶), 139.1 (py-C⁴), 127.6 (py-C³), 125.8 (im), 124.4 (im), 123.6 (py-C⁵), 82.4 (cp), 55.4 (CH₂), 37.8 (CH₃). IR (CH₂Cl₂, cm⁻¹): 1963 ν(CO). Anal. Calcd for C₁₆H₁₆FeN₃O (449.07): C 42.79, H 3.59, N 9.36. Found: C 42.81, H 3.71, N 9.25.

Synthesis of 8b. This complex was prepared from (*N*-isopropyl-*N'*-2-picoly)imidazolium bromide (0.56 g, 2 mmol), KO^tBu (0.29 g, 2.6 mmol), and [FeI(cp)(CO)₂] (0.55 g, 1.8 mmol). The crude product was obtained as a brown powder (0.71 g, 74%). Recrystallization from CH₂Cl₂/Et₂O gave the title compound as orange crystals. ¹H NMR (CDCl₃, 500 MHz): δ 8.82 (dd, 1H, ³J_{HH} = 5.7 and ⁴J_{HH} = 1.4 Hz, py-H⁶), 8.12 (d, 1H, ³J_{HH} = 1.8 Hz, im), 8.08 (d, 1H, ³J_{HH} = 7.8 Hz, py-H³), 7.78 (td, 1H, ³J_{HH} = 7.8 and ⁴J_{HH} = 1.4 Hz, py-H⁴), 7.17 (d, 1H, ³J_{HH} = 1.8 Hz, im), 7.13–7.10 (m, 1H, py-H⁵), 6.52 (low-field part of AX d, 1H, ²J_{HH} = 15.7 Hz, CH₂), 5.53 (high-field part of AX d, 1H, ²J_{HH} = 15.7 Hz, CH₂), 4.76 (s, 5H, cp), 4.55 (septet, 1H, ³J_{HH} = 6.8 Hz, CHMe₂), 1.50, 1.44 (2 × d, 6H, ³J_{HH} = 6.8 Hz, CH(CH₃)₂). ¹³C-{¹H} NMR (CDCl₃, 125 MHz): δ 219.3 (CO), 178.8 (im-C²), 160.0 (py-C²), 159.1 (py-C⁶), 139.1 (py-C⁴), 127.6 (py-C³), 126.5 (im), 123.7 (py-C⁵), 119.0 (im), 82.4 (cp), 55.1 (CH₂), 52.3 (CHMe₂), 23.8, 23.6 (2 × CH(CH₃)₂). IR (CH₂Cl₂, cm⁻¹): 1961 ν(CO). Anal. Calcd for C₁₈H₂₀FeN₃O (477.12) × 1/3 CH₂Cl₂: C 43.57, H 4.12, N 8.31. Found: C 43.48, H 4.36, N 8.62.

Synthesis of 8c. This complex was prepared from (*N*-mesityl-*N'*-2-picoly)imidazolium bromide (0.72 g, 2 mmol), *n*BuLi (1.6 M in hexanes, 1.3 mL, 2 mmol), and [FeI(cp)(CO)₂] (0.55 g, 1.8 mmol). The product was isolated as an orange powder (0.44 g, 44%). Recrystallization of the combined toluene washings from CH₂Cl₂/pentane gave another crop of orange crystals (0.09 g, total yield 53%). ¹H NMR (CDCl₃, 360 MHz): δ 8.80 (d, 1H, ³J_{HH} = 5.4 Hz, py-H⁶), 8.36 (s, 1H, im), 8.16 (d, 1H, ³J_{HH} = 7.2 Hz, py-H³), 7.81 (t, 1H, ³J_{HH} = 7.3 Hz, py-H⁴), 7.13–7.10 (m, 1H, py-H⁵), 7.02, 7.00 (2 × s, 2H, mes-H^{3,5}), 6.96 (s, 1H, im), 6.77 (low-

field part of AX d, 1H, ²J_{HH} = 15.9 Hz, CH₂), 5.70 (high-field part of AX d, 1H, ²J_{HH} = 15.9 Hz, CH₂), 4.57 (s, 5H, cp), 2.36 (s, 3H, *p*-CH₃), 2.00, 1.78 (2 × s, 6H, *o*-CH₃). ¹³C-{¹H} NMR (CDCl₃, 50 MHz): δ 218.6 (CO), 183.1 (im-C²), 160.1 (py-C²), 159.1 (py-C⁶), 139.1 (py-C⁴), 139.9 (mes-C¹), 136.5, 135.5, 134.7 (mes-C^{2,4,6}), 129.7 (mes-C^{3,5}), 129.1 (im), 127.6 (py-C³), 126.6 (im), 125.1 (mes-C^{5,3}), 123.7 (py-C⁵), 82.2 (cp), 55.7 (CH₂), 21.3 (*p*-CH₃), 18.4, 17.9 (2 × *o*-CH₃). IR (CH₂Cl₂, cm⁻¹): 1965 ν(CO). Anal. Calcd for C₂₄H₂₄FeN₃O (553.22): C 52.11, H 4.37, N 7.60. Found: C 52.10, H 4.44, N 7.70.

Synthesis of 9. The procedure was identical to the one described for the synthesis of **6**.

Characterization of 9a. ¹H NMR (acetone-*d*₆, 400 MHz): δ 9.11 (d, 1H, ³J_{HH} = 5.6 Hz, py-H⁶), 7.95 (t, 1H, ³J_{HH} = 7.6 Hz, py-H⁴), 7.74 (s, 1H, im), 7.71 (d, 1H, ³J_{HH} = 7.6 Hz, py-H³), 7.51 (s, 1H, im), 7.30 (t, 1H, ³J_{HH} = 6.6 Hz, py-H⁵), 5.81 (low-field part of AB d, 1H, ²J_{HH} = 15.8 Hz, CH₂), 5.59 (high-field part of AB d, 1H, ²J_{HH} = 15.8 Hz, CH₂), 5.00 (s, 5H, cp), 3.85 (s, 3H, CH₃). IR (CH₂Cl₂, cm⁻¹): 1964 ν(CO).

Characterization of 9b. ¹H NMR (CDCl₃, 360 MHz): δ 8.81 (d, 1H, ³J_{HH} = 5.9 Hz, py-H⁶), 7.78 (m, 3H, py-H³, py-H⁴ and im), 7.16 (d, 1H, ³J_{HH} = 1.8 Hz, im), 7.09 (t, 1H, ³J_{HH} = 5.4 Hz, py-H⁵), 5.85 (low-field part of AB d, 1H, ²J_{HH} = 16.1 Hz, CH₂), 5.42 (high-field part of AB d, 1H, ²J_{HH} = 16.1 Hz, CH₂), 4.73 (s, 5H, cp), 4.56 (septet, 1H, ³J_{HH} = 6.6 Hz, CHMe₂), 1.51, 1.44 (2 × d, 6H, ³J_{HH} = 6.6 Hz, CH(CH₃)₂). IR (CH₂Cl₂, cm⁻¹): 1964 ν(CO).

Characterization of 9c. ¹H NMR (CDCl₃, 500 MHz): δ 8.79 (d, 1H, ³J_{HH} = 5.0 Hz, py-H⁶), 7.97 (br, 1H, im-H), 7.89 (br, 1H, py-H³), 7.81 (br, 1H, py-H⁴), 7.10 (br, 1H, py-H⁵), 7.03, 7.01 (2 × s, 2H, mes-H^{3,5}), 6.97 (s, 1H, im), 6.02 (low-field part of AB, br, 1H, CH₂), 5.61 (high-field part of AB, br, 1H, CH₂), 4.55 (s, 5H, cp), 2.38 (s, 3H, *p*-CH₃), 2.04, 1.80 (2 × s, 6H, *o*-CH₃). ¹³C-{¹H} NMR (CDCl₃, 125 MHz): δ 218.7 (CO), 183.2 (im-C²), 160.2 (py-C²), 159.1 (py-C⁶), 139.3 (py-C⁴), 139.9 (mes-C¹), 136.5, 135.6, 134.8 (mes-C^{2,4,6}), 129.7 (mes-C^{3,5}), 129.1 (im), 127.6 (py-C³), 126.6 (im), 125.1 (mes-C^{5,3}), 123.7 (py-C⁵), 82.3 (cp), 55.6 (CH₂), 21.3 (*p*-CH₃), 18.4, 18.0 (2 × *o*-CH₃). IR (CH₂Cl₂, cm⁻¹): 1966 ν(CO).

DFT Calculations. All DFT calculations have been performed with the parallelized ADF suite of programs, release 2004.01.²⁹ Geometry optimizations were carried out with the generalized gradient approximation, using nonlocal corrections to exchange by Becke³⁰ and to correlation by Perdew³¹ (BP86) The Kohn–Sham MOs were expanded in a large, uncontracted basis set of Slater-type orbitals (STOs), of a triple-ζ + polarization functions quality (TZP), within the frozen-core approximation using a small core for Fe. An auxiliary set of STOs was used to fit the density for the Coulomb-type integrals.^{29a} The IR frequencies are scaled by a factor of 0.953³² using B3LYP³³ geometries with a 6-31G* (C, N, H) basis set and the quasirelativistic LANL2DZ pseudopotentials and basis set for Fe,³⁴ employing the Gaussian 03 suite of programs.³⁵

Bonding analysis of the metal–ligand interactions is accomplished with the extended transition state method (ETS).³⁶ According to the ETS scheme, the bond energy (negative bond dissociation

(29) (a) Baerends, E. J.; Ellis, D. E.; Ros, P. *Chem. Phys.* **1973**, *2*, 41. (b) te Velde, G.; Baerends, E. J. *J. Comput. Phys.* **1992**, *99*, 84. (c) Fonseca-Guerra, C.; Visser, O.; Snijders, J. G.; te Velde, G.; Baerends, E. J. In *MEITECC-9*; Clementie, E., Corongiu, C., Eds.; Cagliari, 1995; p 303. (d) te Velde, G.; Bickelhaupt, F. M.; Baerends, E. J.; Guerra, C. F.; van Gisbergen, S. J. A.; Snijders, J. G.; Ziegler, T. *J. Comput. Chem.* **2001**, *22*, 931.

(30) Becke, A. D. *Phys. Rev. A* **1988**, *38*, 3098.

(31) Perdew, J. P. *Phys. Rev. B* **1986**, *33*, 8822.

(32) Zhou, M.; Andrews, L.; Bauschlicher, C. W. *Chem. Rev.* **2001**, *101*, 1931.

(33) Becke, A. D. *J. Chem. Phys.* **1993**, *98*, 5648.

(34) Hay, P. J.; Wadt, W. R. *J. Chem. Phys.* **1985**, *82*, 270.

energy, BDE) between the two fragments is decomposed in the following interaction terms:

$$\text{Bond Energy} = \Delta E_{\text{tot}} = \Delta E_{\text{prep}} + \Delta E_{\text{Pauli}} + \Delta E_{\text{elstat}} + \Delta E_{\text{oi}} \quad (4)$$

The total interaction energy equals the bond energy and is decomposed into several terms. The first term, ΔE_{prep} , is the energy required to deform the fragments into the geometries they possess in the complex. ΔE_{Pauli} quantifies the Pauli repulsion between the electron densities of the two fragments. The electrostatic attraction ΔE_{elstat} describes the attraction between the nuclei of one fragment and the electron density of the other fragment (vice versa). ΔE_{Pauli} and ΔE_{elstat} are usually summarized as ΔE_{steric} . ΔE_{oi} represents the orbital interaction term, which quantifies the energy gain upon mixing of the orbitals of the two fragments, and is generally dominated by the HOMO–LUMO interactions. This term can be further dissected into the different symmetry classes, which are A' and A'' in the cases we consider here.

Crystal Structure Determinations. Data were collected on a Stoe imaging plate diffractometer system³⁷ equipped with a graphite monochromator. Data collection was performed at -100 °C using Mo $K\alpha$ radiation ($\lambda = 0.71073$ Å). The structures were solved by direct methods using SHELXS-97³⁸ and refined by full matrix least-

squares on F^2 with SHELXL-97.³⁹ The hydrogen atoms were included in calculated positions and treated as riding atoms using SHELXL-97 default parameters. All non-hydrogen atoms were refined anisotropically. No absorption correction was applied for **3b** ($\mu < 1$ mm⁻¹). For all other structures a semiempirical absorption correction was applied using MULABS as implemented in PLATON.⁴⁰ Complex **8b** crystallized with one disordered and partially occupied CH₂Cl₂ molecule (occupancy 0.5 for C37, C11, and C12; occupancy 0.25 for C38, C13, and C14) in the asymmetric unit. The highest final residual electron density in **8b** (2.4 e Å⁻³) was found next to the disordered CH₂Cl₂ molecule. Selected bond lengths and angles and crystallographic details are collected in Tables S1–S4 of the Supporting Information. All calculations and graphical illustrations were performed with the PLATON03 package.⁴⁰ Crystallographic data (excluding structure factors) for the structures **3b**, **5c**, **8a**, **8b**, and **8c** have been deposited with the Cambridge Crystallographic Data Centre as supplementary publication nos. CCDC 614248–644252. Copies of the data can be obtained free of charge on application to CCDS, 12 Union Road, Cambridge CB2 1EZ, UK [fax: (int.) +44-1223-336-033; e-mail: deposit@ccds.cam.ac.uk].

Acknowledgment. We thank Mr. F. Fehr for technical assistance and Prof. R. H. Crabtree for stimulating discussions. M.A. gratefully acknowledges the Alfred Werner Foundation for an Assistant Professorship. This work has been financially supported by the Swiss National Science Foundation (grant 200021-101891).

Supporting Information Available: Crystallographic data for **3b**, **5c**, **8a**, **8b**, and **8c** in CIF format, tables with selected bond lengths and angles, CV of **6a**, and details on the DFT geometry optimization and energy decomposition analysis.

(35) Frisch, M. J.; Trucks, G. W.; Schlegel, H. B.; Scuseria, G. E.; Robb, M. A.; Cheeseman, J. R.; Montgomery, Jr., J. A.; Vreven, T.; Kudin, K. N.; Burant, J. C.; Millam, J. M.; Iyengar, S. S.; Tomasi, J.; Barone, V.; Mennucci, B.; Cossi, M.; Scalmani, G.; Rega, N.; Petersson, G. A.; Nakatsuji, H.; Hada, M.; Ehara, M.; Toyota, K.; Fukuda, R.; Hasegawa, J.; Ishida, M.; Nakajima, T.; Honda, Y.; Kitao, O.; Nakai, H.; Klene, M.; Li, X.; Knox, J. E.; Hratchian, H. P.; Cross, J. B.; Bakken, V.; Adamo, C.; Jaramillo, J.; Gomperts, R.; Stratmann, R. E.; Yazyev, O.; Austin, A. J.; Cammi, R.; Pomelli, C.; Ochterski, J. W.; Ayala, P. Y.; Morokuma, K.; Voth, G. A.; Salvador, P.; Dannenberg, J. J.; Zakrzewski, V. G.; Dapprich, S.; Daniels, A. D.; Strain, M. C.; Farkas, O.; Malick, D. K.; Rabuck, A. D.; Raghavachari, K.; Foresman, J. B.; Ortiz, J. V.; Cui, Q.; Baboul, A. G.; Clifford, S.; Cioslowski, J.; Stefanov, B. B.; Liu, G.; Liashenko, A.; Piskorz, P.; Komaromi, I.; Martin, R. L.; Fox, D. J.; Keith, T.; Al-Laham, M. A.; Peng, C. Y.; Nanayakkara, A.; Challacombe, M.; Gill, P. M. W.; Johnson, B.; Chen, W.; Wong, M. W.; Gonzalez, C.; Pople, J. A. *Gaussian 03*, Revision C.02; Gaussian, Inc.: Wallingford, CT, 2004.

(36) (a) Ziegler, T.; Rauk, A. *Inorg. Chem.* **1979**, *18*, 1755. (b) Ziegler, T.; Rauk, A. *Theor. Chim. Acta* **1977**, *46*, 1.

(37) *X-Area V1.17 & X-RED32 V1.04* Software; Stoe & Cie GmbH: Darmstadt, Germany, 2002.

(38) (a) Sheldrick, G. M. *SHELXS-97*, Program for crystal structure determination; University of Göttingen: Germany, 1997. (b) Sheldrick, G. M. *Acta Crystallogr.* **1990**, *A46*, 467–273.

(39) Sheldrick, G. M. *SHELXL-97*, Program for crystal structure refinement; University of Göttingen: Germany, 1997.

(40) Spek, A. L. *J. Appl. Crystallogr.* **2003**, *36*, 7.